Electrical Power and Energy Systems 62 (2014) 183–188

Contents lists available at ScienceDirect

Electrical Power and Energy Systems

journal homepage: www.elsevier.com/locate/ijepes

A method to enhance the predictive maintenance of ZnO arresters in energy systems

Shyh-Jier Huang *, Chien-Hsien Hsieh

Department of Electrical Engineering, National Cheng Kung University, Tainan 70101, Taiwan

ARTICLE INFO

Article history:
Received 29 May 2013
Received in revised form 12 April 2014
Accepted 16 April 2014

Keywords:
Predictive maintenance
Leakage current
Zinc oxide arrester

ABSTRACT

Leakage current and temperature are common features of zinc oxide (ZnO) arrester degradation in power systems; however, for substation engineers, these key features often bring difficulties in grasping the operating conditions of ZnO arresters because of insufficient maintenance references. Therefore, in this study, the aim is to propose a systematic method to facilitate the realization of predictive maintenance of ZnO arresters in energy systems. The method begins with the feature extraction of ZnO arresters by using on-line resistive current monitoring and infrared radiation (IR) image inspection. A regression model based on the temperature difference, the total leakage current, and the resistive leakage current is then formulated to assist in the insulation diagnosis. This approach is useful to observe the insulation condition, thereby benefiting the predictive maintenance of ZnO arresters. In order to validate the effectiveness of the method, it has been applied to inspect several ZnO arresters installed in a 345 kV substation in Taiwan. Results show that this proposed method performs more effectively than published techniques.

Introduction

Surge arresters are an essential part for the secure operation of power systems. The two primary types of arresters are silicon carbide (SiC) with series gaps and zinc oxide (ZnO) without series gaps. Because ZnO arresters are capable of absorbing high non-linear energy, they are more reliable than SiC arresters and are frequently used in modern power systems [1].

Arresters are usually installed together with power equipment to protect against lightning and switching surges. However, because these arresters contain no gap, they would induce a leakage current that flows through the arrester when a working voltage is applied. The analysis indicated that the leakage currents can be decomposed into a large capacitive current component and a small resistive current one. Normally, the magnitudes of both components are several hundred microamperes and several tens of microamperes [2–4]. Research has shown that the resistive leakage currents often increase in conjunction with insulation degradation. The ZnO material becomes heated when leakage currents increase due to any abnormal condition. Once this generated heat exceeds the dissipation capability of ZnO, a thermal runaway process would immediately take place. This also implies that the leakage current monitoring and thermal inspection serve as effective diagnostic methods for in-service ZnO arresters. Numerous published studies have examined this topic. A wireless passive surface acoustic wave temperature sensor was suggested for measuring the temperature [5]. The resistive current measurement and the influence of harmonics on the measurement were discussed [6,7]. Various diagnostic methods were also mutually compared [8]. The thermal characteristics and thermal stability computation of arresters was used for the protection and maintenance design [9–11]. Some approaches based on the advancement of computational intelligence were also successively developed [12,13]. Previous research revealed that the diagnosis of surge arresters is typically conducted by current measurement or infrared (IR) image inspection, which was considered feasible but lack a concise judging criterion for convenient applications. A further investigation is therefore crucially required.

The study made in this research is aimed to propose a hybrid method combining the leakage current measurement with IR imaging in order to assist the predictive maintenance of ZnO arresters. This approach is proposed based on a regression method that models the relationship between the maximum temperature difference and the resistive leakage current. Through the comprehension of the maximum temperature difference at a specific resistive leakage current, the degradation of the arrester can be early informed once the temperature difference is greater than the predetermined threshold.

* Corresponding author. Tel.: +886 6 2757575 32506; fax: +886 6 234 5482.
E-mail address: clhuang@mail.ncku.edu.tw (S.-J. Huang).

http://dx.doi.org/10.1016/j.ijepes.2014.04.041
0142-0615/

It is note that for a 345 kV system in Taiwan, the arrester is usually formed by a series of three or four sections. Degradation may occur in any section of the arrester, yet the identical leakage currents at each section are incapable of serving as useful discriminator for fault identification. Furthermore, since the maximum surface temperatures seldom differ in a significant manner, which also imply that those existing methods may be ineffective to find the location of abnormal sections. Therefore, the study proposes to utilize the information retrieved from on-line resistive leakage current and IR image inspection, by which the temperature difference, the total leakage current and the resistive leakage current are all collected to analyze, hence enhancing the predictive maintenance capability of arrester. This proposed approach has been effectively applied to real case, by which all abnormal arresters are correctly identified without mismatch. Test results support the feasibility of this method for the application that is investigated.

This paper is organized as follows: Section 'Paradigm and methodology' presents the paradigm and methodology; Section 'Field testing and results' shows the validation of the proposed method; Section 'Discussion' details the findings; and lastly, Section 'Conclusions' offers a conclusion.

Paradigm and methodology

As stated before, the degradation of metal oxide surge arrester in service could occur due to the operating voltage, the impulse currents, and the chemical reactions. The degradation in arrester elements may cause the increment of leakage current, resulting in excessive heat and unexpected aging. The temperature of arrestor column is often a primary basis to justify the operating condition. Yet, because stray capacitances existed in both high and low voltage electrodes which results in an uneven voltage distribution across the arresters, the power loss of arrester elements may not be in proportion to the temperature. Therefore, rather than adopt the maximum temperature, the paper has proposed a temperature difference-based regression analysis for the predictive maintenance of ZnO arresters in this study. Previously, regression analysis is commonly recognized as a useful tool to understand the relations among the variables of concern within the model. This approach allows selected independent variables to be used for forecasting the responses of independent variables. In this equipment maintenance study, a linear regression model developed with Eviews software [14] is employed to determine relationships among maximum temperature difference, total leakage current, and resistive leakage current. The software offers reliable solutions for forecasting applications that have been widely adopted in the field of high-voltage engineering, with satisfactory results [15–18].

Fig. 1 shows the temperature data of a real ZnO arrester that was recorded by the thermal image, where the [1]red line stands for the higher temperature and yellow line the lower temperature measured at different time. This study uses a 69 kV ZnO arrester as a specimen to develop a regression model for the diagnosis of ZnO arresters. The leakage currents and temperatures of ZnO arresters are individually acquired by an online resistive current monitoring system and an IR thermal image [20–22]. Both signals were sampled at one sample per minute over a two-hour period. For the model formulation, the study uses the resistive leakage current and total leakage current as independent variables, whereas the maximum temperature difference is deemed as a dependent variable. A multiple regression model can be therefore expressed as

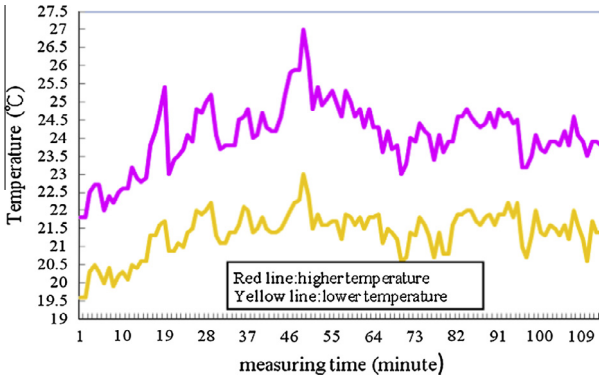

Fig. 1. Temperature inspection of a real ZnO arrester.

$$Y_i = \beta_0 + \beta_1 X_1 + \beta_2 X_2 + \varepsilon_i \quad (1)$$

where Y_i is the maximum ZnO temperature difference, X_1 is the resistive leakage current variable, X_2 is the total leakage current variable, $\beta_1$is the coefficient of the resistive leakage current, β_2 is the coefficient of the total leakage current, β_0 is the Y-intercept, and I is the random error. The coefficients in (1) are determined by the least-squares method, whereas the p-value test provides a measure of interdependence among these variables. A smaller p-value represents a greater dependency. Note that the dependent variable is closely related to a specific independent variable when its p-value is less than 0.05, indicating that both variables come with a significant positive correlation. Greater details on statistical theory can be found in [19]. The developed regression model is investigated as follows.

In this model, the dependent variable is maximum temperature difference (Y), and the independent variables are resistive leakage current (X_1) and total leakage current (X_2). Table 1 shows the regression analysis results of these variables. The values of the coefficients $\beta1$, $\beta2$, and $\beta0$ are 0.022669, 0.000540, and −0.388186, respectively. The regression equation can be hence derived as

$$Y = 0.022669X_1 + 0.000540X_2 - 0.388186 \quad (2)$$

The degree of correlation (p = .0008) between Y and X_1 is significantly less than the threshold (p = .05), implying hat Y and X_1 have a significant positive correlation [23–24]. It is worth mentioning here that X_2 is also related to Y because their correlative degree (p = .3742) indicates that X_2 is negligible in this study.

The analysis and discussion shows that the maximum temperature difference (Y) on the IR inspection is significantly relevant to the resistive leakage current (X_1) of the arrester. A statistical model based on this key variable (X_1) is presented to understand its significance. The model is convenient for further applications because it requires only one variable.

Table 2 shows the results of the second regression model. The values of the coefficients $\beta1$ and $\beta0$ are 0.024050 and −0.043203, respectively. The regression function equation can be expressed as

$$Y = 0.024050X_1 - 0.043203 \quad (3)$$

Table 1
Result of regression Model I.

	Max. temperature difference (Y)	p-value
Resistive leakage current (X_1)	0.022669 (3.435263)	.0008
Total leakage current (X_2)	0.000540 (0.892118)	.3742
Y-intercept	−0.388186 (−0.346089)	.7299

[1] For interpretation of color in Figs. 1 and 2, the reader is referred to the web version of this article.

Table 2
Result of regression Model II.

	Maximum temperature difference	*p*-value
Resistive leakage current (X_1)	0.024050 (3.752702)	.0003
Y-intercept	−0.043203 (−0.04107)	.9673

The degree of correlation between Y and X_1 (p = .0003) confirms a significant positive correlation. The analysis shows that the ZnO arrestor's maximum temperature difference has a significant relationship with the resistive leakage current. This provides a practical one-to-one relationship between Y and X_1. As shown in (3), for a given resistive leakage current (X_1) of a ZnO arrester, its maximum temperature difference (Y) can be estimated through this formulated model. Fig. 2 shows the recorded maximum temperature differences and their corresponding estimated values obtained from (3), where a total number of 116 points are delineated. In the figure, the red line represents the estimated values, and the blue line represents the measured ones. The range of percentage errors for each record is about 4–6%. It is known that an increment of resistive leakage current results in large power losses and the heating of ZnO element, causing the arrester to deteriorate rapidly. The resulting maximum temperature difference is a useful diagnostic feature. The diagnostic rule is that a greater maximum temperature difference of arresters indicates a larger degree of degradation. Although a diagnosis standard is not yet commonly recognized, the proposed model establishes a gauge of maximum temperature difference that is beneficial for making reasonable decisions for predictive maintenance. The computed values and on-site measurements also reached a good agreement.

Field testing and results

Fig. 3 shows a block diagram of on-line resistive leakage current monitoring system. An on-line resistive leakage current monitoring with infrared imaging (IR) constructs a diagnostic tool for the field test. The analysis of leakage current harmonics is made based on a compensation technique, where the third-order harmonic current generated by system voltage is eliminated such that only the third-order current component generated by the surge arrester is solely calculated. The third-order harmonic resistive current (I_{3r}) is obtained from the total third-order harmonic current (I_{3t}) subtracted from the capacitive third-order harmonic current (I_{3c}), which is expressed as $I_{3r} = I_{3t} - I_{3c}$. The total leakage current is measured by means of the zero-flux current transformer, and the electric field is measured in terms of the current induced in the field probe. The compensation is made by the simultaneous

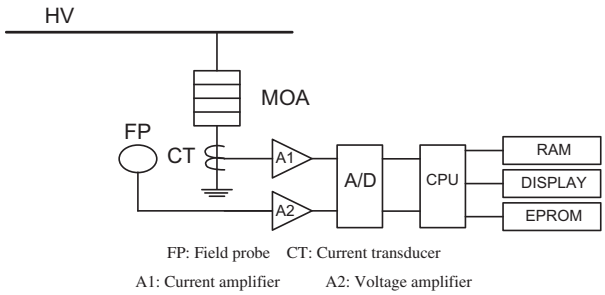

Fig. 3. ZnO arrester on-line leakage current monitoring diagram.

measurements of total leakage current of MOA and the current induced in a field probe [8,9].

Fig. 4 shows the temperature of ZnO arrester measured by infrared imaging (IR) detectors that is a non-invasive monitoring. The temperature measurement is made once per minute, and the resistive current is measured each 10 min. Three 288 kV ZnO arresters were served as test samples to validate the effectiveness of the proposed method. These arresters were installed in a 345 kV substation in central Taiwan. Each arrester is composed of four sections that are connected individually with a different phase of the three-phase power system. The arresters were monitored through on-line leakage current measurement and IR image acquisition. For each monitoring specimen, both the highest and the lowest temperature were taken, by which the relative temperature difference is used as an aid to comprehend the condition of the MOA. Note that the temperature of ZnO arrester is slightly higher than the ambient temperature in order to maintain the thermal equilibrium. It was found that the temperature difference between ZnO and the ambient temperature is about 3.6–7.2 °C at noon, and 1.6–3.3 °C at night. This also indicates that the temperature influence to the ZnO is more significant in a sunny day.

In addition, we have also made measurements of resistive leakage currents and evaluated their temperature variations. Table 3 shows the monitoring results of resistive current and thermal imaging for ZnO arresters. As the table tabulates, the resistive leakage current of three phases are 370.7 μA in the R-phase, 337 μA in the S-phase, and 289.4 μA in the T-phase. The resistive leakage current flowing through each section is identical because each arrester is formed with four sections that are connected in a series.

Proposed method

This study presents a regression model to offer a judgment criterion for the predictive maintenance of ZnO arresters. By substituting the values of these resistive currents into (3), the thresholds of the maximum temperature differences for different arresters are 8.9 °C for the R-phase, 8.1 °C for the S-phase and

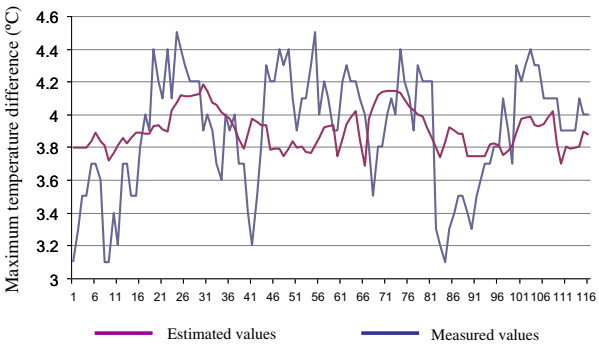

Fig. 2. Maximum temperature difference of estimated values and measured ones.

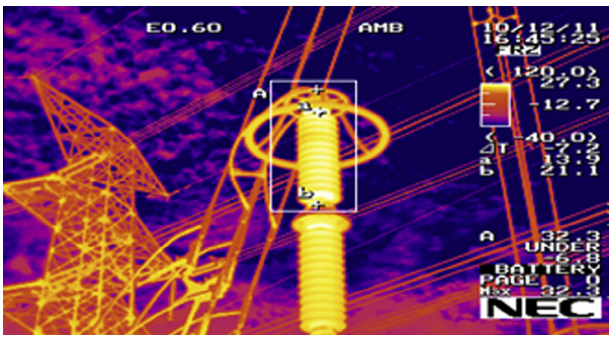

Fig. 4. Detection of arrester temperature using IR images.

Table 3
Monitoring of resistive current and thermal imaging for ZnO arresters.

Specimen	Resistive current (μA)	Maximum temperature (°C)	Minimum temperature (°C)	Maximum temperature difference (°C)
R_Φ				
Section 1	370.7	32.3	19.3	13.0
Section 2		28.7	23.1	5.6
Section 3		25.3	21.5	3.8
Section 4		23.4	20.2	3.2
S_Φ				
Section 1	337.0	30.6	18.6	12.0
Section 2		26.9	19.2	7.7
Section 3		21.5	17.5	4.0
Section 4		21.3	17.7	3.6
T_Φ				
Section 1	289.4	27.6	18.4	9.2
Section 2		24.4	17.7	6.7
Section 3		20.6	16.5	4.1
Section 4		22.9	17.1	5.8

Table 4
Proposed criterion for ZnO arresters diagnosis.

Specimen	Resistive current (μA)	Values of maximum temperature difference		Diagnostic results
		Proposed criterion (°C)	Measured value (°C)	
R_Φ				
Section 1	370.7	8.9	*13.0*	Poor
Section 2			5.6	–
Section 3			3.8	–
Section 4			3.2	–
S_Φ				
Section 1	337.0	8.1	*12.0*	Poor
Section 2			7.7	–
Section 3			4.0	–
Section 4			3.6	–
T_Φ				
Section 1	289.4	6.9	*9.2*	Poor
Section 2			6.7	–
Section 3			4.1	–
Section 4			5.8	–

6.9 °C for the T-phase. These temperature differences represent the threshold of insulation conditions of different arresters. For a convenient comparison, Table 4 tabulates the threshold values and measured values, where the symbol "–" indicates that the temperature difference is acceptable. By observing this table, the insulation condition of Section 1 R-phase arrester is found to be poor since the measured temperature difference of 13 °C is larger than the threshold of 8.9 °C. Prudent attentions are hence suggested for such measurement, anticipating providing an effective measure to enhance the predictive maintenance of arresters.

Comparisons of methods

To validate the proposed method, a power outage was arranged and the tested arresters were removed for an off-line electrical test. The test contains measurements of insulation resistance and power losses. Table 5 summarizes these results, where the lower values of insulation resistance corresponds to a greater power loss and indicates a poor insulation. In this study, for those arresters with the power loss exceeding the 150 mw, they are deemed poor ones. This threshold was determined based on the discussions utility engineers along with field test experience.

Next, the study provides a comparison of the proposed approach with the decision rule of IR image inspection. The

Table 5
Results of insulation test and power loss measurement.

Specimen	Measured insulation resistance (MΩ)	Power loss Measured value (mw)	Diagnostic results
R_Φ			
Section 1	2500	164	Poor
Section 2	10,000	115	–
Section 3	25,000	103	–
Section 4	25,000	101	–
S_Φ			
Section 1	2500	162	Poor
Section 2	25,000	117	–
Section 3	25,000	90	–
Section 4	25,000	104	–
T_Φ			
Section 1	3000	156	Poor
Section 2	20,000	95	–
Section 3	25,000	99	–
Section 4	25,000	70	–

Table 6
Result of temperature difference inspection.

Specimen	Maximum temperature difference in percent $\triangle T$		Diagnostic results
	Criterion (%)	Measured $\triangle T$ (%)	
R_Φ			
Section 1	30	*40.2*	Poor
Section 2		19.5	–
Section 3		15.1	–
Section 4		13.7	–
S_Φ			
Section 1	30	*39.2*	Poor
Section 2		28.6	–
Section 3		18.6	–
Section 4		16.9	–
T_Φ			
Section 1	30	*33.3*	Poor
Section 2		27.5	–
Section 3		19.9	–
Section 4		25.3	–

maximum temperature difference obtained by thermal imaging is expressed in a percentage form

$$\Delta T(\%) = \frac{T_1 - T_2}{T_1} \times 100\% \quad (4)$$

where ΔT is the percentage of temperature difference, T_1 is the maximum temperature, and T_2 is the minimum temperature of an IR image. As a standard measure in Taiwan, the diagnosis threshold is set at 30%. Table 6 shows the percentage temperature difference obtained using (4). It shows that the differences for Section 1 of various arresters are greater than the criterion of 30%, whereas the remaining sections are lower than 30%. Based on the designated rule, the abnormal sections are correctly detected. These comparisons show that the proposed method is in agreement with previous experiences, facilitating the predictive maintenance of arresters.

Discussion

The on-line resistive current measurements conducted in this study may be impacted by environmental conditions and harmonic contents in the power system because measurements are made on outdoor field equipment along with a high electric field. Therefore, in addition to this on-line resistive current measurement system, a portable leakage current meter with reliable anti-interference capabilities is also employed to measure the leakage current and

Table 7
Compared table of resistive leakage current measurements.

Specimen	Direct measurement values			On-line monitoring values			Error (%)
	1st (μA)	2nd (μA)	Avg. (μA)	1st (μA)	2nd (μA)	Avg. (μA)	
Location I							
R_Φ	129.3	129.4	129.3	114	115	114.5	11.4
S_Φ	150.6	151.2	150.9	138	146	142.0	6.0
T_Φ	102.5	97.7	100.1	96	94	95	5.1
Location II							
R_Φ	41.6	41.5	41.6	48	46	47	13.0
S_Φ	31.9	32.4	32.2	38	36	37	14.9
T_Φ	40.6	42.7	41.7	50	46	46	10.3
Location III							
R_Φ	168.6	170.7	169.6	165	167	166	2.1
S_Φ	143.8	137.0	140.4	140	136	138	1.7
T_Φ	85.7	89.4	87.5	84	86	85	2.9

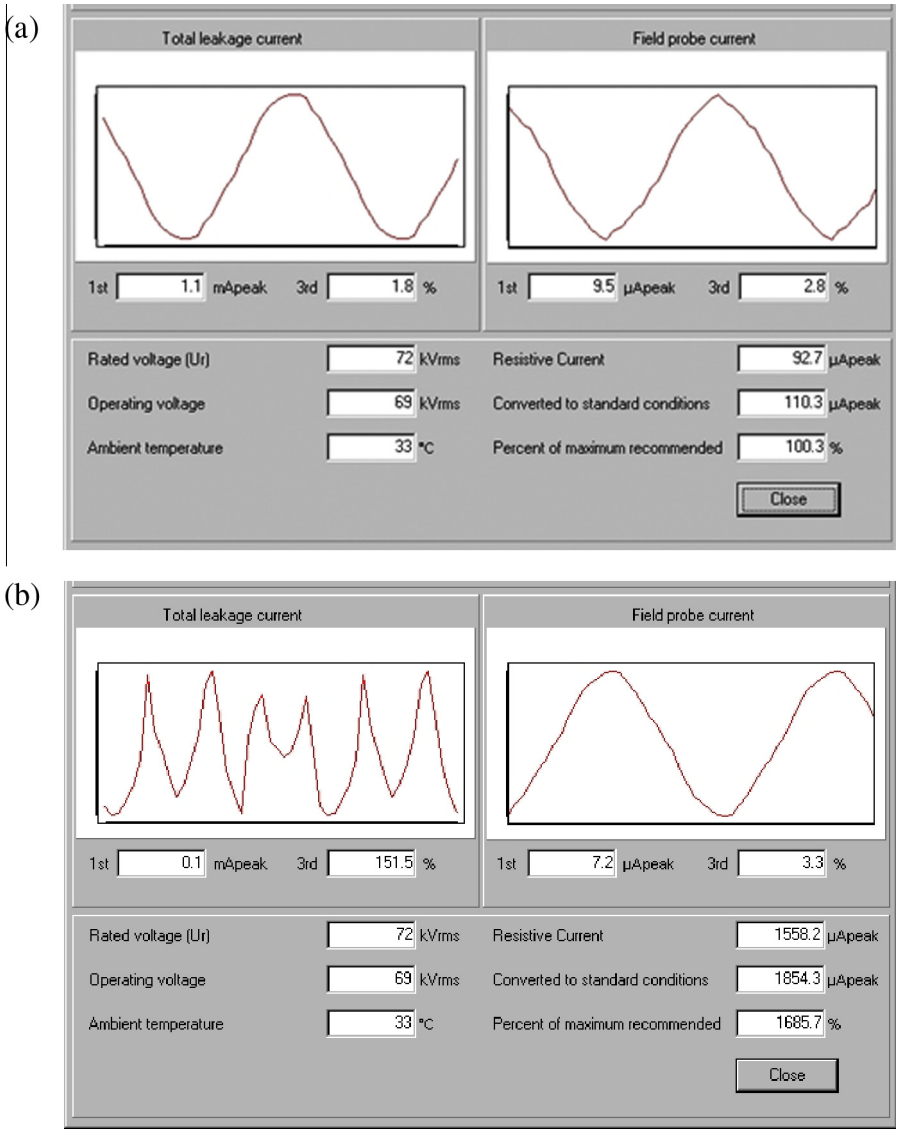

Fig. 5. Effects of magnetic and radio frequency interference on the total leakage current.

examine the accuracy of the on-line monitoring. The readings from the portable meter are served as direct measurement values, whereas the readings from the on-line monitoring system are used as on-line measurement values. The percentage error is consequently obtained.

A total of nine ZnO arresters installed in three different locations were selected as test samples. Each sample was measured twice by the on-line system and portable meter. Test results are listed in Table 7, which shows that the percentage errors between them are within 15%. It is seen that most of errors are lower than

10%, implying that the accuracy of the on-line monitoring system is acceptable.

The factors that affect IR image inspection and on-line leakage current monitoring are discussed below.

The influencing factors on the accuracy of IR inspection

Inspection of IR imaging is effective for detecting abnormal heat generation. Yet, the inspection accuracy may be affected by several external factors such as wind, solar flux, high load, and seasonal factors. To ensure a correct judgment, the IR image measurement should avoid adverse weather conditions. Besides, the emissivity (ε) of this equipment is known to be highly dependent on the surface and material of an object. For example, black objects require the ε value to be set at 1 to obtain accurate results, while the ε value is smaller than 1 for colored objects. Prudent attentions are suggested to be paid on the proper understanding of the emissivity coefficient before those measurements are made.

Influencing factors on the accuracy of leakage current monitorin

On-line leakage current monitoring is often affected by two types of disturbances: harmonic interference and radio frequency interference (RFI). In practice, measurement results are acceptable if the ratio of the third harmonic component to the fundamental component is smaller than 5%. However, for the effects of RFI, they are relatively difficult to quantify. Fig. 5(a) and (b) shows the examples of these impacts on the measurement results. The waveform on the left of Fig. 5(a) presents a reasonable measured value of total leakage current (1.1 mA) when the supply voltage contains an acceptable third harmonic component of 1.8%. The waveform on the left of Fig. 5(b) shows another experimental result with the supply voltage that consists of the third harmonic component of 151.5%. The figure shows that the measured value of total leakage current of 0.1 mA, while the current waveform has encountered a significant distortion.

The impact of RFI on the monitoring of resistive leakage current is certainly worthy of discussion. The resistive leakage current was labeled "field probe current" in Fig. 3. The measured value of resistive leakage currents under different temperatures can be standardized to a value that corresponds to a condition of 20 °C, as shown in Fig. 5. The waveforms on the right of Fig. 5(a) and (b) shows examples of third harmonic components of 2.8% and 3.3%, respectively. Although the third harmonic components in these cases are smaller than 5%, the measured results are enormously different. The waveform on the right of Fig. 5(a) indicates the resistive leakage current value of 92.7 μA at a temperature of 33 °C (or 110.3 μA when converted to a condition of 20 °C); yet with a strong RFI interference, the waveform on the right of Fig. 5(b) becomes an unreasonable value of 1558.2 μA (or 1854.3 μA when converted to a condition of 20 °C). In order to ensure measurement accuracy, these unexpected factors should be all properly taken into consideration.

Conclusions

Monitoring of leakage current and thermal variation is beneficial as a predictor of early stage insulation deterioration, thereby serving as useful aid for predictive maintenance of ZnO surge arresters. In view of this critical importance, the study proposed an approach of enhancing the predictive maintenance of ZnO arresters. By using on-line resistive leakage current monitoring and IR image inspection, the paper suggested a regression model-based fault-diagnosis in ZnO arresters, by which a diagnostic work can be systematically formed. Rather than solely rely on the experience of engineers, the method has includes the statistical analysis such that a better inference results can be better ensured. This method is not only capable of solving the case when arresters consist of several sections connected in series, but also justifies the insulation degradations of individual sections which may not be diagnosed effectively using traditional methods. This method is currently being validated on more arresters under different configurations. We will also take the seasonal factor into considerations when discussing the temperature difference between ZnO and the ambient temperature at different times. Test results will be reported in the near future.

Acknowledgment

The authors are grateful for the technical assistance from the Electrical System Department at Taiwan Power Company.

References

[1] Yan X, Wen Y, Yi X. Study on the resistive leakage current characteristic of MOV surge arresters. In: IEEE/PES transmission and distribution conference and exhibition, vol. 2. Tokyo, Japan; October 2002, pp. 683–87.
[2] Zhao T, Li Q, Qian J. Investigation on digital algorithm for on-line monitoring and diagnostics of metal oxide surge arrester based on an accurate model. IEEE Trans Power Delivery 2005;20(2):751–6.
[3] Korendo K, Florkowski M. Thermography based diagnostic of power equipment. Power Eng J 2001;15(1):33–42.
[4] Wong KL. Electromagnetic emission based monitoring technique for polymer ZnO surge arrester. IEEE Trans Dielectr Electr Insul 2006;13(1):181–90.
[5] Hinrichsen V, Scholl G, Schubert M, Ostertag T. Online monitoring of high-voltage metal-oxide surge arresters by wireless passive surface acoustic wave (SAW) temperature sensors. In: International symposium on high voltage engineering. London, England; August 1999, pp. 238–41.
[6] Chrzan K, Koehler W. Diagnostics of high-voltage metal-oxide surge arresters procedure errors. In: International symposium on high voltage engineering. London, England; August 1999, pp. 385–88.
[7] Zhu H, Raghuver MR. Influence of representation model and voltage harmonics on metal oxide surge arrester diagnostics. IEEE Trans Power Delivery 2001;16(4):599–603.
[8] Heinrich C, Hinrichsen V. Diagnostics and monitoring of metal-oxide surge arresters in high-voltage networks- Comparison of existing and newly developed procedures. IEEE Trans Power Delivery 2001;16(1):138–43.
[9] Stockum FR. Simulation of the nonlinear thermal behavior of metal oxide surge arresters using a hybrid finite difference and empirical model. IEEE Trans Power Delivery 1994;9(1):306–13.
[10] He J, Zeng R, Chen S, Tu Y. Thermal characteristics of high voltage whole-solid-insulated polymeric ZnO surge arrester. IEEE Trans Power Delivery 2003; 18(4):1221–7.
[11] Zhong Z, Boggs SA, Imai T, Nishiwaki S. Computation of arrester thermal stability. IEEE Trans Power Delivery 2010;25(3):1526–9.
[12] Laurentys Almeida CA, Braga AP, Nascimento S, Paiva V, Martins HJA, Torres R, et al. Intelligent thermographic diagnostic applied to surge arresters: a new approach. IEEE Trans Power Delivery 2009;24(2):751–7.
[13] Neto ETW, da Costa EG, Maia M. Artificial neural networks used for ZnO arresters diagnosis. IEEE Trans Power Delivery 2009;24(3):1390–5.
[14] Eviews 7.0. IHS Global Inc., Colorado, USA.
[15] Flynn MJ, Sarkani S, Mazzuchi TA. Regression analysis of automatic measurement systems. IEEE Trans Instrum Meas 2009;58(10):3373–9.
[16] Jauregui-Rivera L, Xiaolin M, Tylavsky DJ. Improving reliability assessment of transformer thermal top-oil model parameters estimated from measured data. IEEE Trans Power Delivery 2009;24(1):169–76.
[17] Moser G, Serpico SB. Modeling the error statistics in support vector regression of surface temperature from infrared data. IEEE Geosci Remote Sens Lett 2009;6(3):448–52.
[18] Li J, Sun C, Sima W, Yang Q, Hu J. Contamination level prediction of insulators based on the characteristics of leakage current. IEEE Trans Power Delivery 2010;25(1):417–24.
[19] Freund JE. Modern elementary statistics. New Jersey, USA: Prentice Hall; 2007.
[20] Stojanovic ZN, Stojkovic ZM. Evaluation of MOSA condition using leakage current method. Electr Power Energy Syst 2013;52:87–95.
[21] Valsalal P, Usa S, Udayakumar K. Response of metal oxide arrester in gas-insulated substation and method to improve its dynamic characteristics. IET Sci Meas Technol 2012;6(4):222–8.
[22] Pinto AG, Costa EM, Kurokawa S, Monteiro JA, Franco J, Pissolato J. Analysis of the electrical characteristics and surge protection of EHV transmission lines supported by tall towers. Electr Power Energy Syst 2014;57:358–65.
[23] Bakar A, Talib D, Mokhlis H, Illias HA. Lightning back flashover double circuit tripping pattern of 132 kV lines in Malaysia. Electr Power Energy Syst 2013;45:235–41.
[24] Zhou N, Pierre JW, Trudnowski D. A stepwise regression method for estimating dominant electromechanical modes. IEEE Trans Power Delivery 2012;27(2):1051–9.